World Electric Vehicle Journal

MDPI

Review

A Review of Sealing Systems for Proton Exchange Membrane Fuel Cells

Yi Wei, Yanfeng Xing *, Xiaobing Zhang, Ying Wang, Juyong Cao and Fuyong Yang

School of Mechanical and Automotive Engineering, Shanghai University of Engineering Science, Shanghai 201600, China; m310122468@sues.edu.cn (Y.W.); wangyingcae@sues.edu.cn (Y.W.); 01180010@sues.edu.cn (J.C.); yangfy@sues.edu.cn (F.Y.)

* Correspondence: xyf2001721@sues.edu.cn

Abstract: The sealing technology of proton exchange membrane fuel cells (PEMFCs) is a critical factor in ensuring their performance, impacting driving safety and range efficiency. To guarantee the safe operation of PEMFCs in complex environments, it is essential to conduct related sealing research. The structure of the fuel cell sealing system is complex, with components in close contact, and identifying factors that affect its sealing performance is crucial for the development and application of the cells. This paper briefly describes the sealing mechanism of PEMFCs and introduces four typical sealing structures. It considers both the assembly and operation processes, summarizing assembly errors, sealing gaskets, and sealing leaks as well as vibration, cyclic temperature and humidity, and cyclic assembly. The research status of the sealing system in simulations and experiments is reviewed in detail. The key factors affecting the sealing performance of fuel cells are emphasized, highlighting the significance of dynamic detection of the gasket status, stack performance improvement under cumulative errors, and multi-objective optimization models combining contact pressure with the characteristics of stack components.

Keywords: proton exchange membrane fuel cell; new energy vehicles; sealing structure; assembly technology

Citation: Wei, Y.; Xing, Y.; Zhang, X.; Wang, Y.; Cao, J.; Yang, F. A Review of Sealing Systems for Proton Exchange Membrane Fuel Cells. *World Electr. Veh. J.* **2024**, *15*, 358. https://doi.org/10.3390/wevj15080358

Academic Editor: Michael Fowler

Received: 2 July 2024
Revised: 29 July 2024
Accepted: 5 August 2024
Published: 9 August 2024

1. Introduction

Due to the global energy crisis and the pollution caused by burning fossil fuels, clean energy has become the focus of attention worldwide [1,2]. Vigorous development of new energy vehicles, led by electric vehicles, has become our national strategy as well as an international consensus. Hydrogen energy is the cleanest energy in the world, it is flexible, abundant, and conducive to sustainable development, and it can also be used for long-distance transport operations and the development of energy-consuming industries [3]. The proton exchange membrane fuel cell (PEMFC) is an electrochemical device that converts hydrogen energy into electricity with high power density, high conversion efficiency, zero emissions, and low noise [4]. Compared to other types of fuel cells, the PEMFC is able to operate in dry or low relative humidity conditions [5], and it is typically an "environmentally friendly" fuel. The PEMFC has a variety of fuel sources and can also use fuels such as methanol [6]. Therefore, the PEMFC is considered to be a good choice for replacing conventional fuel engines, but its material cost and manufacturing cost are high. Its main fuel source, hydrogen, is more difficult to prepare and store [7]. Therefore, the PEMFC is considered to be a good choice to replace the traditional fuel engine. The PEMFC mainly consists of end plates, insulating plates, a collector, a bipolar plate (BPP), gaskets, and membrane electrodes. Among them, the BPP and membrane electrodes, as the core components of the fuel cell, have been research hotspots in the current field, compared to which the sealing materials and performance of the cell are neglected research objects [8]. However, in the overall structure of the fuel cell, serious safety hazards arise due to the emergence of dimensional and shape errors in various components, as well

as the occurrence of sealing structure failure during assembly or startup, resulting in the mixing or leaking of reactant gases. Therefore, the stability of the cell sealing is crucial to the performance and safety of the electric reactor. Major automotive companies around the world have been conducting high-cost and long-term research and development on hydrogen fuel cells, and the number of papers on the topic of cell sealing has been increasing year by year, as shown in Figure 1. Ye et al. [9] of Wuhan University of Technology outlined the types of sealing structures for membrane electrode assemblies (MEAs) of PEMFCs, pointing out that the sealing-frame-wrapped membrane electrode type is more convenient in terms of electric stack assembly and that the rigid protective frame sealing structure has a broader application prospect. Qiu et al. [10] from Shanghai Jiao Tong University reviewed the effect of pressure on sealing from the aspect of power reactor assembly technology, derived the concept of seal degradation from the form of gasket degradation, and outlined the improvement model of sealing structure. Considering the importance of sealing in the assembly and use of fuel cells, as well as the emergence of various new methods and technologies in recent years, it is crucial to reflect the development of this field in a more comprehensive and timely manner. In this paper, a systematic review is made on the sealing research of PEM fuel cells, focusing on the influence of the assembly components and process on the sealing performance of the battery. The aim of this paper is to sort out and summarize the existing simulation experiments, with a view to generating new sealing technologies, which can ultimately promote the development of sealing research on PEM fuel cells.

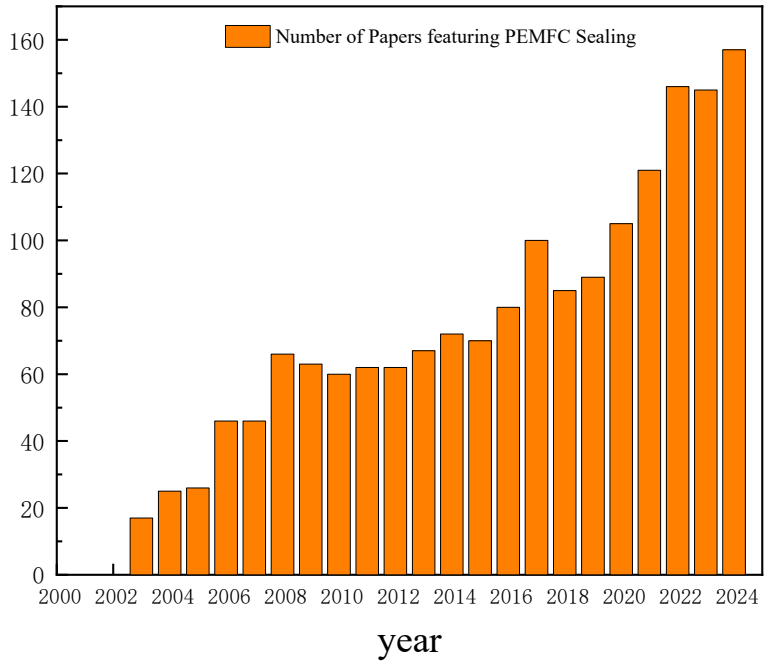

Figure 1. Number of papers with PEMFC sealing as the topic.

2. Sealing Mechanism of Proton Exchange Membrane Fuel Cell

As a direct power source of new energy vehicles, the performance of the PEMFC will directly affect the power, economy and recognition of new energy vehicles. Figure 2 shows that [11] is the typical structure of PEMFC, and it consists of end plates, insulating plates, a collector, a BPP, and membrane electrodes. The basic unit of the fuel cell presents a sandwich form: BPP–membrane electrodes–BPP. The membrane electrode assembly consists of proton exchange membranes (PEM), a gas diffusion layer (GDL), and a catalyst layer (CL).

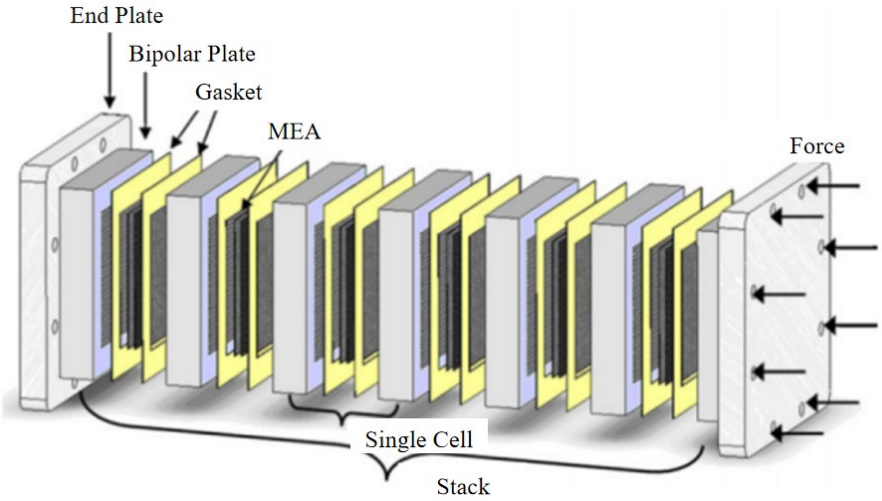

Figure 2. PEMFC structure composition. Reprinted with permission from Ref. [11]. Copyright 2022 Elsevier.

Fuel cell stacks are made of several single-cell stacks, and there are many factors restricting the power of fuel cell stacks, but improving the overall sealing is a prerequisite for fuel cell performance improvement. The overall sealing performance of the stack depends on the sealing effect of the seals between the graphite plate and the membrane electrodes, and the sealing material must have a certain stability and durability under humid, acidic, and high-temperature environments [12,13]. If the sealing material is degraded by the chemical reaction in the fuel cell, the hydrogen in the flow channel will be in direct contact with the air, mixing together or leaking, which will lead to a serious safety problem [14]. Rubber is usually chosen as the sealing material for fuel cells.

The roughness of the sealing parts is also an important factor affecting the sealing performance of the battery; based on Persson's rough surface penetration theory [14], the surface of any two precision objects may not be able to maintain a complete and stable seal. Under microscopic conditions, the surface of any object is non-smooth. As shown in Figure 3, the contact surface of the two objects can be seen after magnification of the contact surface of the existence of peaks and valleys. These surface gaps can lead to leakage of reaction gases or liquids in fuel cells [15]. Persson rough surface gap permeability theory based on Poiseuille fluid theory [16,17] and Stauffer–Aharony Persson rough surface gap permeation theory is based on Poiseuille fluid theory and Stauffer–Aharony through flow theory ζ [18] to quantitatively represent the leakage rate. Persson in the rough surface contact mechanics theory creatively introduces the amplification rate and defines the contact pressure probability density function related to the amplification rate as $P(p, \zeta)$; the function $P(p, \zeta)$ in the definition domain can be obtained by integrating the current amplification rate of the real contact area $A(P_0, \zeta)$ and the ratio of the theoretical contact area A_0. The calculation equation is as follows [19,20]:

$$\frac{A(p_0, \zeta)}{A_0} = \int_0^{+\infty} P(p, \zeta) dp = \mathrm{erf}\left(\frac{p_0}{2\sqrt{G}}\right) \quad (1)$$

$$P_0 = \frac{F}{A_0} \quad (2)$$

G in Formula (1) is the elastic rough surface topography parameter; P_0 is the nominal contact stress, the value of which is known by the contact pressure F compared with the nominal contact area A_0, calculated as shown in Formula (2); and $\mathrm{erf}(.)$ represents the Gaussian error function.

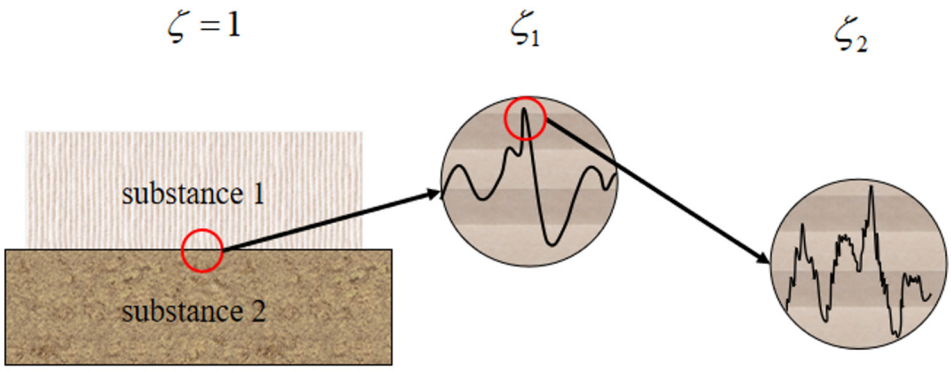

Figure 3. The morphology of the contact surface of the object at different magnifications.

The leakage rate Q per unit time through a specific contact area $(L_x \times L_x)$ along the x-direction is as follows [16,17]:

$$Q = \alpha \frac{L_y}{L_x} \cdot \frac{u_1^3(\zeta, q_0, q_1)}{12\eta} \Delta P \quad (3)$$

In Equation (3), α is the leakage channel factor, u_1 represents the height of the leakage channel, q_0 represents the minimum number of waves that can be detected by the experiment, q_1 represents the maximum number of waves that can be detected by the experiment, η is the viscosity of the fluid, and ΔP represents the difference in pressure on both sides of the leakage channel. If the amplification ζ is known, the leak rate Q can be derived.

Persson's rough surface penetration theory states that when the ratio of the real contact area $A(p_0, \zeta)$ to the theoretical contact area A_0 is 0.4 or less, the rough contact surface forms a leakage channel and the fuel cell seal fails.

3. Seal Structure Design

According to the sealing mechanism and sealing materials of PEMFCs, researchers have carried out a large number of performance analyses of the electric stack [21–35] and optimized the design of the cell structure [23–35]. The currently commonly used sealing structures of PEMFCs can be categorized into four types [9,24,25].

3.1. Direct Sealed Frame

The sealing gasket in the direct-seal structure is compressed on both sides of the permeation membrane in the inactive region, and the sealing ring is compressed by external load to achieve the sealing function, and the BPP with flow channels separates the gas from the anode and cathode. As shown in Figure 4 [9], Yoshida et al. [26] utilized a double sealing mode: the sealing gasket is compressed directly on the permeation membrane to prevent gas from permeating outward, forming the first seal; the sealing ring is compressed between the membrane electrode and the BPP to prevent gas from leaking outward, forming the second seal. The direct seal structure is simple, easy to disassemble frequently, and can withstand small loads. This structure requires high performance of the permeation membrane and sealing gasket. Since the sealing material and permeation membrane are in direct contact, the sealing material should be selected as a neutral material that is highly durable and will not cause damage to the membrane.

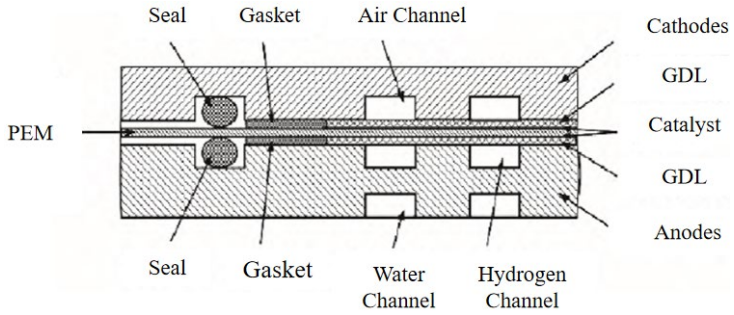

Figure 4. PEM direct sealing structure. Reprinted with permission from Ref. [9]. Copyright 2013 Elsevier.

3.2. Rigid Wrapped Frame

A rigid wrapped frame refers to a structural whole after the rigid frame at the edge of the membrane electrode structure is compressed and combined with other sealing materials or thermoplastic materials [9,27–31]. The rigid wrapped frame can provide some sealing effect after compression; its structure and dimensions have a significant influence on the compression rate of the membrane electrode after the assembly of the electrostack. Its rigid material and sealing material determine the minimum contact resistance between the membrane electrode and the BPP; and at the same time, it can protect the membrane electrode from being damaged by excessive compression during operation. As shown in Figure 5 [9], Xu et al. added a protective layer on both sides of the PEM. The material of the protective layer may be polytetrafluoroethylene for waterproofing and air permeability. Adding a rigid frame to the outside of the protective layer produces little compression damage, but reactive gases can also overflow from the frame gaps. Therefore, it is necessary to add rubber sealing gaskets to the surface of the rigid frame to enhance the sealing. The rigid wrapped frame needs to use a variety of rigid materials and sealing materials. Its size and structure also plays a key role in the performance of the battery cell; therefore, to complete the overall assembly, the rigid wrapped frame components need to have an accurate size and structure.

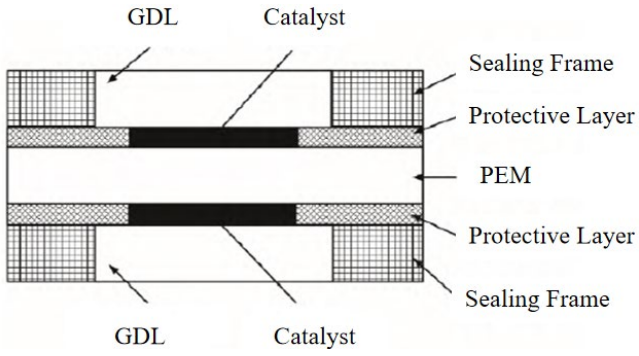

Figure 5. Rigid protective frame sealing structure. Reprinted with permission from Ref. [9]. Copyright 2013 Elsevier.

3.3. Seal Wrapped Proton Exchange Membrane Type Frame

The sealed outer side of the PEM is wrapped by a sealing material that can be bonded, and the two BPPs close to the PEM are also connected by the sealing material, which, together with the GDL and the flow field plate, form a single-crystal module. As shown in Figure 6 [9], the seal wrapped around the PEM type generally adopts a plastic frame to fix the outer side of the PEM with a mold, and then it is injection molded and becomes the main sealing element after cooling [32]. After injection molding, the seals are integrated with the PEM, which is beneficial to prevent the reaction gas from penetrating into the

cathode or anode and at the same time prevent the reaction gas from leaking to the outside world, which is conducive to the stacked assembly and mass production of the power reactor, but it is difficult to disassemble and reassemble. The use of different injection molding materials for the sealing structure can reduce the contact resistance, optimize the contact pressure, and enhance the overall effectiveness of the stack.

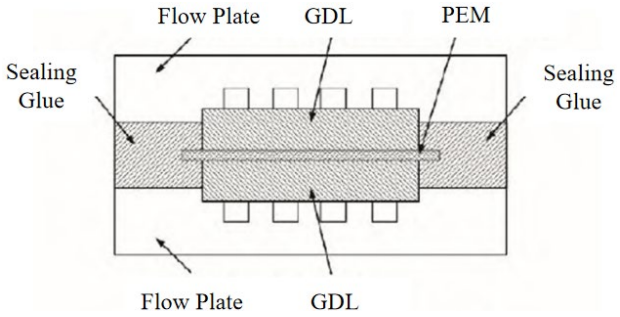

Figure 6. PEM-wrapped frame sealing structure. Reprinted with permission from Ref. [9]. Copyright 2013 Elsevier.

3.4. Seal-Wrapped Membrane Electrode-Type Frame

Similar to the seal-wrapped PEM-type frame, the membrane electrode honeycomb region in the seal-wrapped membrane electrode-type frame structural form is wrapped with an adhesive-able sealing material that includes a GDL, anode catalyst, cathode catalyst, and PEM. To further improve the sealing, Wozniczka et al. used an adhesive to connect the membrane electrode edge sealing region to the flow field plate sealing region to form a flow-shaped sealing member, forming a second seal. As shown in Figure 7 [9], in order to maintain the sealing of the cell while further improving the performance of the cell, Jacobine [32] used a light-curing sealing material as a sealant, and after the injection molding was completed, the sealing material penetrated into the catalyst and GDL to form a soft-sealing frame-type integrated membrane electrode structure. It is worth noting that under the working pressure and temperature of the cell, the sealing material will melt and penetrate into the porous media of the GDL and the catalyst layer. The connection between the membrane electrode frame and the sealing frame will become tighter and more evenly loaded. Sealant wrapping the membrane electrode frame to form an integrated membrane electrode structure is conducive to stacked assembly and mass production of power stacks, but sealant directly wrapped around the edge of the membrane electrode will make the disassembly and reassembly of the core difficult.

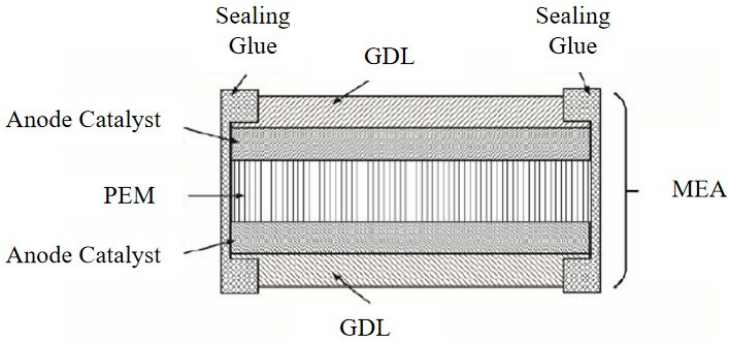

Figure 7. MEA-wrapped frame sealing structure. Reprinted with permission from Ref. [9]. Copyright 2013 Elsevier.

At present, it seems that the fuel cell industry has not formed a unified sealing structure, and the four mainstream sealing structures have their own advantages and characteristics that can be applied to different experimental scenarios. Direct-seal frames are suitable

for applications that do not require high-pressure seals, and they are relatively simple and inexpensive to design and manufacture, despite moderate power densities; however, improper installation can result in poor localized seals, and gasket materials may deteriorate over time, leading to seal failure. The rigid wrapped frame is mechanically compressed to realize sealing, which can maintain a better sealing effect in high-temperature and high-pressure as well as corrosive environments, and is commonly used in high-performance fuel cell vehicles, such as the Hyundai NEXO; however, it requires precise mechanical design and installation, and the cost is high. The seal-wrapped membrane electrode-type frame is characterized by high adaptability and high power density and is commonly used in underwater or aerospace scenarios [33]. Its structure is able to maintain sufficient stability in extreme temperatures and chemical environments, but its equipment and technology costs are high, and it is not easy to dismantle and replace it after a leak occurs. The seal-wrapped membrane electrode-type frame has good sealing performance and excellent corrosion resistance. Stable at high temperatures and in a wide range of chemical environments, they have a high power density and are suitable for industrial applications and high-power-output devices; again, they require precise temperature control and complex processes, and are difficult to maintain.

Conventional PEMFCs have BPPs and membrane electrodes that are independently fabricated and assembled under assembly pressure and then sealed against oxygen, hydrogen, and coolant by seals, making the wire-seal structure easy to process and simple to visualize. However, there are manufacturing errors between components and single seals, and the force stability of the reactor is poor during long-term operation, which makes it difficult to ensure the consistency of the whole reactor. Yin Jun et al. [34] from Tongji University proposed an integrated sealing design as shown in Figure 8a, in which the BPP and the membrane electrode are formed into a single component by injection molding, and the sealant infiltrates into the GDL to ensure the parallelism and distance between the membrane electrode and the BPP on both sides. As shown in Figure 8b, the function of the 1–14 protruding platform on the pole plate is to fix the membrane electrode, protect the carbon paper from being excessively compressed, and ensure the flatness between the two plates. The height d of the tab on the polar plate is calculated as follows:

$$d = b_{GDL} \times (1 - f_{r1}) + b_{CL} \times (1 - f_{r2}) + C - b_{Fr} \quad (4)$$

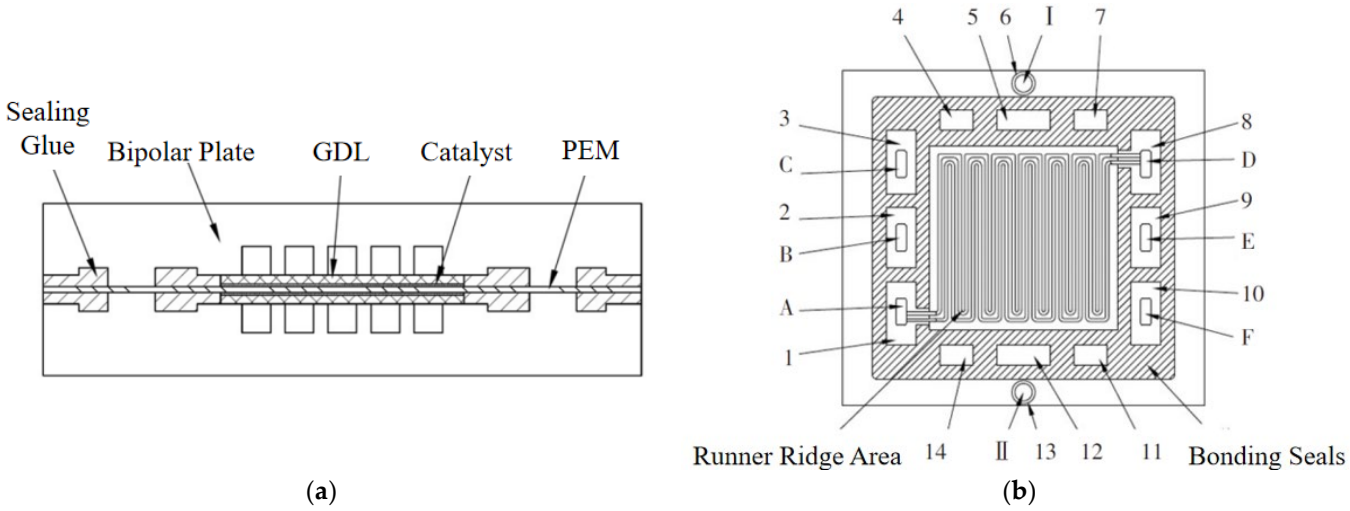

(**a**) (**b**)

Figure 8. Schematic of integrated seal structure: (**a**) schematic of integrated sealed single-cell structure; (**b**) schematic plan view of an integrated sealed single cell: 1–14. protruding platform; A–F. intake and exhaust manifold holes and coolant holes; I, II: positioning holes. Reprinted with permission from Ref. [8]. Copyright 2021 IEEE Xplore.

In Equation (4), b_{GDL} is the original thickness of the GDL on the same side as the polar plate; b_{CL} is the original thickness of the CL on the same side as the polar plate; f_{r1} and f_{r2} denote the compression rates of the GDL and CL on the same side as the polar plate, respectively; C is the depth of the sealing groove; and b_{Fr} is the thickness of the resin framework.

The integrated sealed single cell adopts a face sealing structure, and the resin frame is uniformly wrapped around the membrane electrode, which can also avoid the phenomenon of stress concentration under the working condition of a large temperature difference. In addition, the process ensures the safety of the cell and prevents the reaction gas and coolant from leaking out.

4. Factors Affecting the Sealing of the Battery in the Assembly Process

As shown in Figure 9, the sealing performance of the PEMFC is mainly affected by the assembly error of each component, the shape of the seal ring, and the sealing groove during the assembly process. The following content is centered on the above three influencing factors.

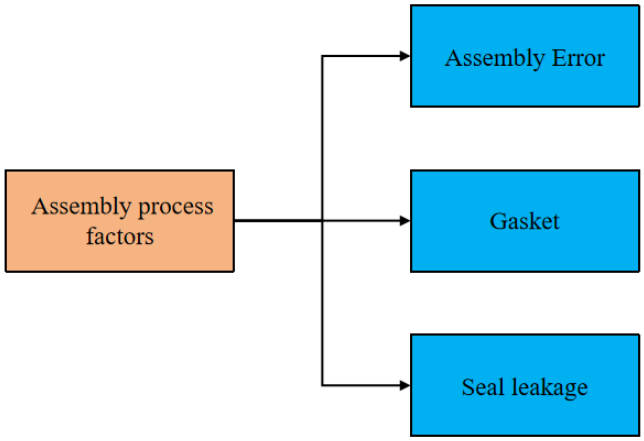

Figure 9. Influencing factors in the assembly process.

4.1. Assembly Error

In the assembly process of the electric stack, the BPPs, membrane electrodes, and sealing gaskets are sequentially clamped. During the clamping process, the intrinsic properties and contact characteristics of the individual elements of the mono-cell are affected. As shown in Figure 10 [35], the misalignment of the BPP is one of the main factors affecting the sealing performance of the cell and causes sealing failure. Firstly, the metal BPP has a pin hole size error in the stamping process, which will directly lead to the displacement deviation between components in the PEMFC assembly, which is an unavoidable problem. Secondly, the metal BPP will rebound during the stamping process, and welding thermal deformation will occur during the subsequent welding process, both of which will directly lead to shape error of the metal BPP and exacerbate the misalignment between neighboring BPPs. Liang et al. [35] defined the concepts of slip distance and slip angle to evaluate the sealing failure model in the PEMFC, and the literature pointed out that the slip angle of the metal BPP is significantly larger than that of the graphite BPP. The slip distance also increases with the increase in hardness, and thicker membrane electrode frames and BPPs with lower hardness are beneficial to ensure the stability and reliability of the seal structure.

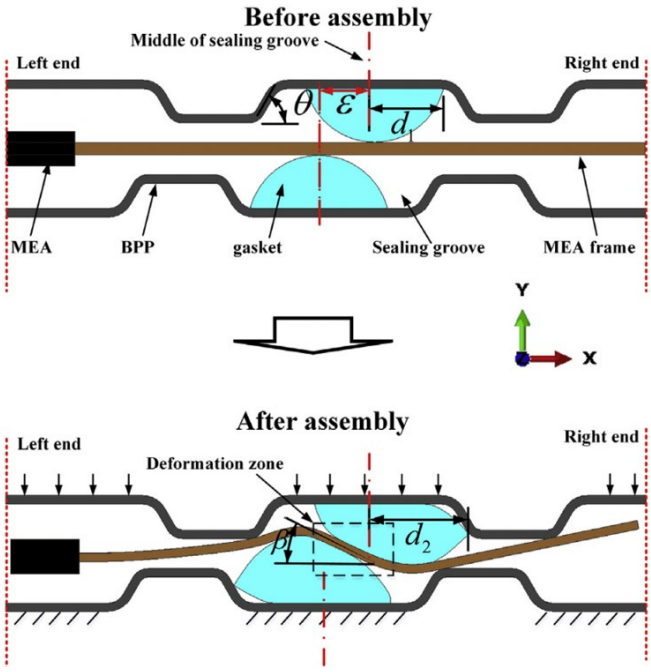

Figure 10. Seal gasket sliding due to misalignment of BPP. Reprinted with permission from Ref. [35]. Copyright 2017 Elsevier.

The manufacturing process of the core and the material of the BPP are important factors affecting the shape of the sealing groove. Graphite BPPs have relatively low hardness and are usually machined by milling or rolling. Therefore, the shape of the sealing groove is related to the shape of the tool, which has a rectangular cross-sectional shape, and the vertical sidewalls are favorable for the contact between the sealing gasket and the BPP, which provides a good sealing effect [36]. The sealing groove of metal BPP is commonly made through a stamping process [37–39], and its sealing groove shape is trapezoidal with rounded corners [40]. As shown in Figure 10, the larger the sealing groove sidewall angle θ is, the higher the probability of sealing failure, and the sealing gasket will slide out of the sealing groove. A representative study was conducted by Habibnia et al. [22], who investigated the effect of effective parameters such as clamping force, end plate thickness, and seal groove depth on the uniform pressure of the GDL on the basis of leakage tests. By means of experiments and finite element simulations, they firstly conducted sealing tests under no-leakage conditions to obtain the minimum compressive stress of the gasket, and then investigated the effective parameters of each component when uniformly distributed pressure was obtained by GDL. The test results show that increasing the depth of the sealant groove leads to an increase in the pressure on the GDL; the increase in the depth of the groove on the BPP indicates that the minimum compressive stress of the gasket becomes smaller, and the increase in the clamping force leads to an increase in the pressure on the GDL, which also raises the likelihood of leakage from the power stack system. A thicker end plate allows for an even distribution of GDL pressure.

4.2. Gasket

The sealing gasket is located in the sealing groove of the BPP, which is the first component under pressure during the assembly of the PEMFC, and can achieve effective sealing for the adjacent BPP, and the thickness of the sealing gasket is greater than the height of the flow field channel. In order to achieve effective sealing, the sealing gasket should have certain properties: appropriate hardness, reasonable mechanical strength, excellent thermal and chemical stability, and good relaxation properties. When an assembly load is applied to the stack, the stress on the gasket should be less than the yield limit of the sealing material, so the sealing determines the minimum assembly load of the stack [9]. The durability

of the gasket is an important factor affecting the sealing performance of the electrostack; Tan et al. [41] investigated the chemical degradation and mechanical degradation of silicone rubber materials under constant assembly load, as shown in Figure 11, where gasket samples and Plexiglas panels were placed in polypropylene vials containing an ADT solution, and an assembly load was applied to the gasket samples. The samples were placed at temperatures of 60 °C and 80 °C for testing, and every 1 or 2 weeks, the samples were removed for weight change monitoring and surface changes to the gaskets were observed using an optical microscope. The results showed that the higher the operating temperature of the gaskets, the faster their degradation rate and the worse their sealing performance.

In addition, many researchers have conducted PEMFC electrostack aging tests to investigate the effects of operating temperature, operating vibration, compression rate, catalyst, reaction gases, and acidic environments on the performance of the gaskets in order to predict gasket life [42–46]. Studies have shown that harsh operating conditions can cause the sealing gaskets to eventually rupture. Cleghorn et al. [47] found, in a three-year battery life test, that the thickness of the silicone rubber gaskets was reduced by approximately 25 μm, and gasket degradation was very evident at the edges of the cell's active region, which not only degraded the cell's sealing performance but even increased the contact resistance of the GDL, leading to a reduction in the overall efficiency of the cell. From a microscopic point of view, BPP and gaskets are ultrathin, making it difficult to obtain leakage rates experimentally [48]. Yang et al. [49] developed a mapping model between the microscale contact behavior and macroscale leakage rate. The sealing performance of the whole interface was analyzed through the self-imitation and self-similarity properties between the gasket and the BPP, which were not available in the traditional macroscopic studies. Thus, the leakage rate of the PEMFC interface was quickly analyzed and predicted.

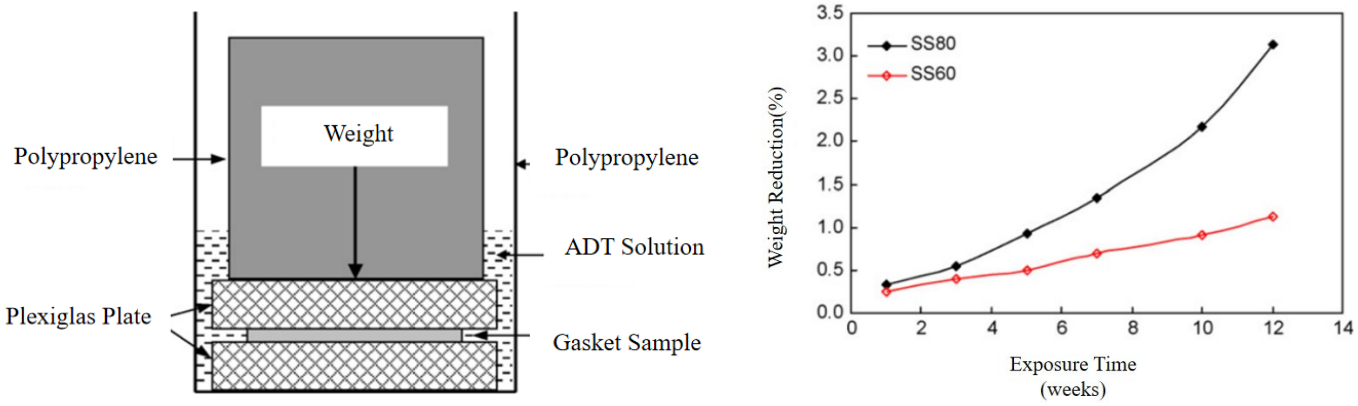

(**a**) (**b**)

Figure 11. Gasket degradation under constant load: (**a**) schematic diagram of compression load test; (**b**) weight loss of gasket samples at 60 °C and 80 °C for different exposure times. Reprinted with permission from Ref. [41]. Copyright 2017 Elsevier.

4.3. Seal Leakage

Interfacial leakage due to rough surface contact and gas permeation in the sealing structure are the main research objects at present, and the gas travelling from one end to the other in the sealing structure mainly occurs at the junction between the gasket and the BPP or the membrane electrode frame. Both interfacial leakage and gas permeation phenomena are closely related to the contact pressure, and the uniformity of the contact pressure is usually used as one of the evaluation criteria for sealing of the electrostacks [50], and in practice, interfacial leakage and gas permeation often occur simultaneously [51]. In PEMFC stacks, the interface area of the gasket between the BPP and the membrane electrode in contact with the reactive gas is very large, and the higher operating temperature of the stack will inevitably affect the overall safety in the case of most stacks using rubber as the

sealing gasket. Husar et al. [52] investigated the overall performance of a seven-section fuel cell stack and found that sealing leakage led to an abnormal change in temperature and pressure of the single leaking cell, which led to an increase in the overall temperature and pressure. Thus, the temperature of the overall electric stack rises and seal failure eventually occurs.

Chen et al. [53] adopted a conventional test method to perform a pressure test to investigate the gas leakage rate and overall electrochemical characteristics of PEMFCs under different assembly torques. Increasing the assembly torque can improve the sealing performance of the electrostack, but the flow channel in the metal BPP is deformed due to the reduced porosity and hydrophobicity of the GDL. Excessive torque reduces the stack sealing and thus the overall power. For softer materials, leakage was determined using the bubble emission method [54] by placing the cell in equilibrium at room temperature with a vacuum gauge, an inlet tube from a vacuum source, and an outlet tube connected to the atmosphere. Since the gas permeability is too small to be detected by traditional measurement methods, Xu et al. [55] used helium mass spectrometry to measure the leakage of the electrostack at different contact pressures and differentiated the interfacial leakage and gas permeation of the gaskets by the difference of the steady-state flow and the stabilization process between the flow channels. In order to make the sealing performance of the electrostack more stable, the effects of interfacial leakage and gas permeation should be taken into account during assembly.

5. Factors Affecting the Sealing of the Battery during Operation

As shown in Figure 12, the sealing performance of a PEMFC is mainly affected by vibration, dynamic compression, and cyclic temperature and humidity during operation. The following content is centered on the these influencing factors.

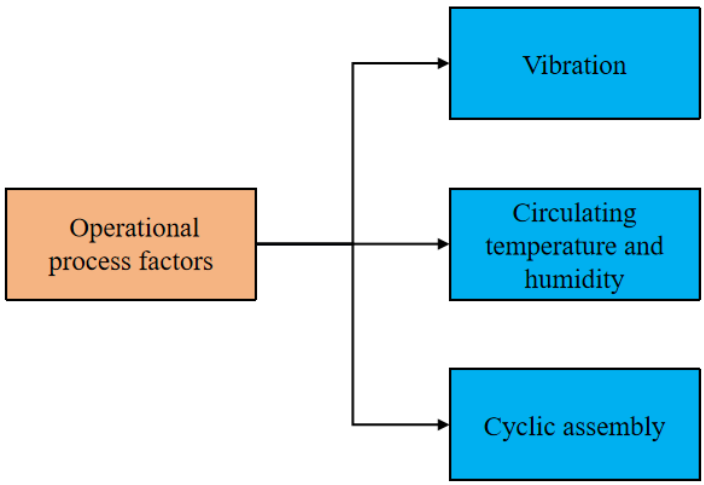

Figure 12. Influencing factors during operation.

5.1. Vibration

Due to the presence of rough surfaces, automotive fuel cells are inevitably subjected to vibration and shock loads during operation, and the stacks generate compressive and excessive shear stresses [56]. The forces generated by vibration are random and difficult to regulate quantitatively. Hou et al. [57] studied the airtightness change in fuel cell stacks under prolonged vibration using a 150 h intensive vibration test, and measured the airtightness change of the stacks of 560 cells under the condition of 50 kPa of pressure; the result was that the hydrogen leakage rate was increased by 50%, which was due to the destruction of the internal sealing structure of the reactor as a result of long-term vibration. As shown in Figure 13, Deshpande et al. [58] detected the resonance at the edge of the gasket using finite element analysis and obtained the location of the possible hydrogen

leakage (Figure 13b). Through further investigation, it was found that the torque of the bolts near the point of resonance was about 75% of the original torque, and the contact pressure started to increase with vibration. Therefore, it was found that the gasket leakage rate increased as the vibration intensified (Figure 13a). Rajalakshmi et al. [59] conducted vibration tests on the PEMFC power pile under considered operating conditions; they found that the change in vibration frequency affects the change in bolt torque, which was reduced by 20% within a frequency range of 50–150 Hz, and, hence, the overall sealing of the power pile was also enhanced.

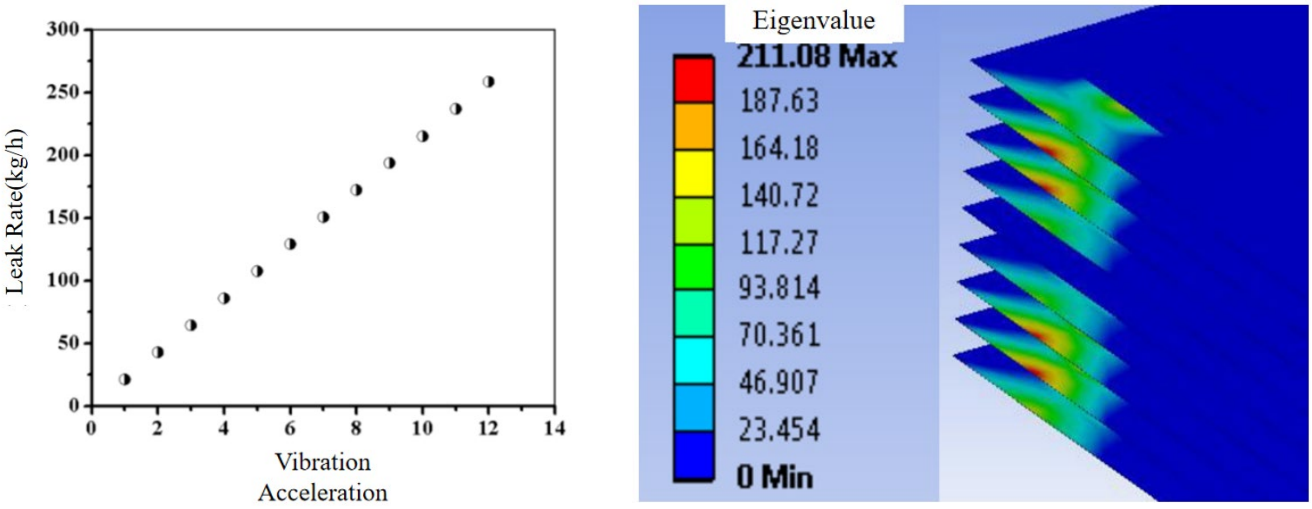

Figure 13. Influence of vibration on the sealing of the electric stack under finite element analysis: (**a**) hydrogen leakage rates at different vibration accelerations; (**b**) stress analysis of the electric stack assembled with 10 cells. Reprinted from Ref. [58].

5.2. Circulating Temperature and Humidity

Under the actual working condition, a chemical reaction occurs inside the fuel cell stack after operation, temperature and humidity increase but remain within a reasonable range, and the fuel cell undergoes a cooling and drying process after the end of operation. As a result, thermal expansion and cooling contraction occur continuously in the stack; in the long run, the sealing of the stack will be reduced and leakage will occur, affecting its efficiency and even causing safety accidents. Husar et al. [52] investigated the data reasons for the failure of a seven-cell fuel cell stack subjected to temperature, pressure, and other variables leading to the failure of the stack. Figure 14 shows the variation in pressure and temperature with time; Figure 14a shows the peak in temperature as the pressure decays (between 16:30 and 16:40). The temperature of the electrostack reaches 91 °C when the internal pressure cannot be maintained, and the test is forced to terminate. Figure 14b indicates the time versus pressure and core temperature between 15:50 and 16:10. At 16:05 the load is removed, temp1–3 increases, and temp4–8 decreases, suggesting that the main factor in the failure of the electrostack is the increase in temperature due to thermal cycling.

As mentioned in the previous section, Liang et al. [35] found that the seal failure in the electric stack is due to the fact that the gaskets cannot be installed in the corresponding positions completely and accurately during the assembly process, and misalignment will inevitably occur after assembly. They further found that the thermal expansion of the sealing gaskets may lead to slippage or even slip outside the sealing grooves when the temperature rises, which will lead to the failure of the fuel cell stack. In addition to this, studying the relationship between temperature and gaskets from a chemical point of view, Cui et al. [60] concluded that thermal expansion or contraction is the main source of compressive stress in seals, and that sealing loads are released as the temperature cycles.

This is because the deformation of silicone rubber originates from the free rotation of the chemical bonds on the long molecular chains and the sliding caused by the sliding between the molecular chains. Once the temperature increases, more external heat is provided to the free rotation of the chemical bonds, and the friction between the molecular chains decreases, so the cycling temperature accelerates the stress relaxation of the sealing rubber material and reduces the sealing of the electrostack. Taehyeong Kim et al. [61] took a different approach; they observed the temperature and relative humidity under the operating condition of the power pile and analyzed the transient behavior of the temperature and water distribution within the active region of the PEMFC while considering the time factor. Thus, the temperature and relative humidity inside the PEMFC will change immediately during acceleration and deceleration. The stability, durability, and sealing of the stack system will be affected to some extent at this moment.

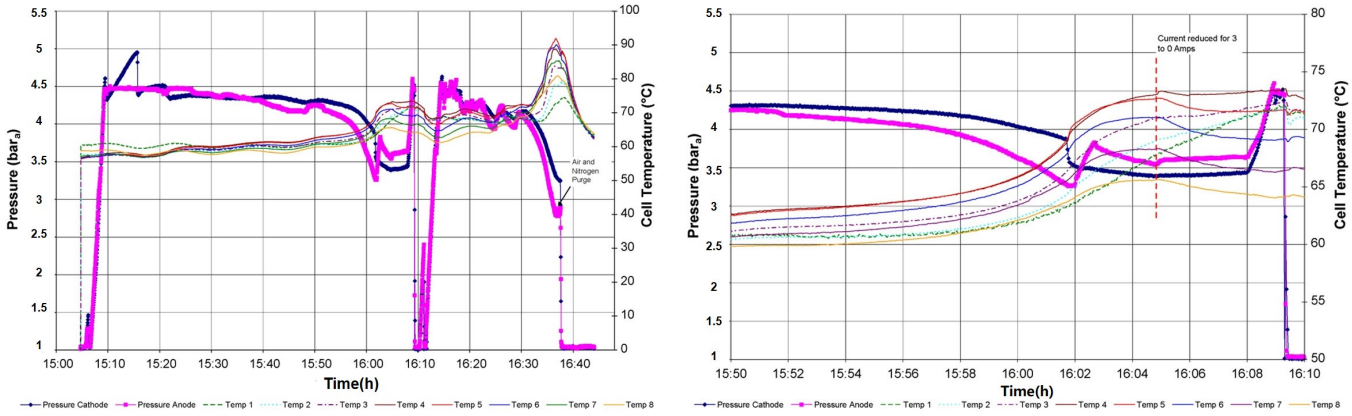

Figure 14. Variation in core temperature and pressure with time: (**a**) pressure of the reactant gasses vs. cell temperature during the last hours of operation; (**b**) expanded view of (**a**) between 15:50 and 16:10. Reprinted with permission from Ref. [52]. Copyright 2007 Elsevier

5.3. Cyclic Assembly

PEMFC may experience cell short circuits, seal leaks, and component misalignment under real-world conditions, and the stack is then disassembled and reassembled repeatedly to ensure the performance of the PEMFC. Therefore, the BPPs, membrane electrodes, gas diffusion layer (GDL), and gaskets in the stack are subjected to cyclic compression forces: the peak pressure is reached after the stack is assembled, and the pressure is released after the stack is disassembled. The geometrical and mechanical properties of the GDL are difficult to recover from cyclic compression forces, and the efficiency of the stack is affected to some extent, and sealing failures may occur under cyclic pressures. Zhang et al. [62] analyzed the compression ratio, fluid pressure, and temperature of the PEMFC based on the thermo-mechanical coupling model. The effects of the compression ratio, fluid pressure, and temperature on the sealing performance of PEMFC were analyzed, and they found that when the three factors are elevated, the contact pressure of the gasket increases, its deformation is intensified, the von Mises stress increases, and the sealing performance of the power reactor is better. Zhang et al. [63] investigated the sealing characteristics of polytetrafluoroethylene (PTFE) as a sealing gasket material under cyclic compression force, and it was shown that the pressure release lags behind the pressure assembly, forming a hysteresis loop. In the pressure release stage, the seal leakage rate of cyclic unloading lags behind cyclic loading, which can improve the sealing performance of the power reactor. The seal leakage rate is positively correlated with the compression force. Focusing on the interior of a single cell, Pei et al. [64] removed the excess water on the membrane electrode by changing the air intake of the cathode and utilizing the cyclic variable pressure to obtain the cell performance under different cyclic variable pressures, currents, and cell

temperatures. As shown in Figure 15, the maximum water removal rate of the cathode is 99.25% under ideal conditions, and the reduction in water content can effectively enhance the sealing of the electric stack and improve the overall performance of the stack.

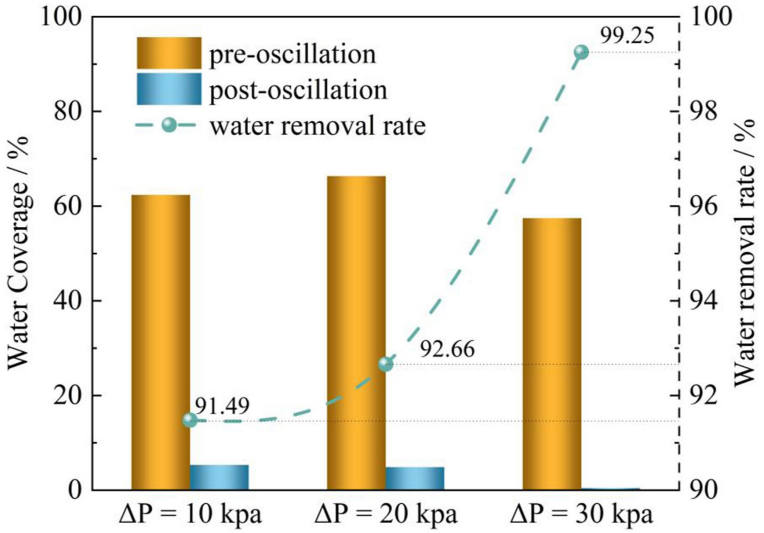

Figure 15. Variation in water coverage at different pressure pulsation amplitudes during the first variable pressure cycle. Reprinted with permission from Ref. [64]. Copyright 2024 Elsevier.

6. Conclusions

This paper first gave a brief description of the sealing mechanism of PEMFC, and then introduced four typical sealing structures and their applications under different working conditions. Then, the factors affecting the sealing of the cell during the assembly process were described in detail from the three aspects of assembly error, sealing gasket, and sealing leakage, and the factors affecting the sealing of the cell during the operation process were elaborated from the three aspects of vibration, cyclic temperature and humidity, and cyclic assembly, and the relevant literature was collated and reviewed, pointing out the problems in the research of the PEMFC sealing. From this the following main conclusions are drawn:

(1) Progress has been made in the research of cell sealing structure, and a new sealing structure has been developed on the basis of the original traditional structure; however, no cell sealing structure is universal, but should be selected based on the specific application conditions. The electric reactor unit is a stacked structure composed of multiple materials and components, and it mainly relies on the improvement of the area of the cell reactant and the number of stacked layers to increase the efficiency of the electric reactor, and the enhancement of the performance of the individual components as well as the improvement of the fit of the components are key to enhancing the sealing of the fuel cell electric reactor. Enhancing the performance of individual components and improving the fitness of each component are key to enhancing the sealing of fuel cell stacks.

(2) Ensuring the good performance of the sealing gasket during assembly and operation is the key factor to ensure the safety, stability, and high efficiency of the fuel cell. In the static state when the fuel cell is not in operation, it is necessary to minimize the assembly error of each component, especially the BPP and the sealing gasket, and control the size of the assembly pressure so that it is kept in a reasonable interval to make the sealing stable. When the fuel cell is in operation, different parts made of different materials will be aged, and the reduction in gasket thickness is the most typical behavior. That said, few articles have mentioned how to detect the gasket status during operation. Therefore, a mechanism that detects the state of components in real time during operation and adjusts them dynamically is a future research direction. Sealing materials age and degrade during long-term operation and need to resist the effects of harsh environments such as high temperature and acidity. Therefore, high-performance polymers and nanocomposites will

be the focus of future seal material research. New materials with superior performance are also accompanied by high costs; the use of additive manufacturing technology and manufacturing complexity combined may be one of the future development trends.

(3) Considering the working environment of the fuel cell, the performance of the single cell and the assembly precision of the stack should be controlled in the design and manufacturing process, so as to avoid sealing leakage and thus reduce the probability of cyclic compression force generated by repeated disassembling and assembling. In recent years, more and more research has taken into account the stress and strain, the contact behavior of components, etc., and controlling the size of contact pressure has become another key way of sealing the power reactor. Currently, there is no complete analytical model that can accurately combine the contact pressure with the characteristics of each component; thus, in the future, it is also necessary to implement a multi-objective optimization method to balance the various indexes, in order to achieve the best sealing effect. With the development of artificial intelligence, the combination of sensing technology and intelligent control is used. Thus, real-time monitoring of the state of the sealing system as well as repairing and optimizing the operation and design of the sealing system are also important for significantly improving the reliability of the PEMFC sealing system.

Author Contributions: Conceptualization, Y.W. (Yi Wei) and Y.X.; methodology, Y.W. (Yi Wei); validation, X.Z.; investigation, F.Y.; resources, Y.W. (Ying Wang); writing—original draft preparation, Y.W. (Yi Wei); writing—review and editing, Y.W. (Yi Wei) and Y.X.; supervision, J.C.; funding acquisition, Y.X. All authors have read and agreed to the published version of the manuscript.

Funding: This research received no external funding.

Data Availability Statement: No new data were created or analyzed in this study. Data sharing is not applicable to this article.

Acknowledgments: I would like to thank all the teachers and students in the lab for their support and help. I hope we can work together in the future to achieve our dreams!

Conflicts of Interest: The authors declare no conflict of interest.

References

1. Jia, Y.H.; Qi, Z.L.; You, H. Power production enhancement with polyaniline composite anode in benthic microbial fuel cells. *J. Cent. South Univ.* **2018**, *25*, 499–505. [CrossRef]
2. Liu, G.; Liu, T.; Wei, Z.; Zhang, Q. Effects of different poses and wind speeds on flow field of dish solar concentrator based on virtual wind tunnel experiment with constant wind. *J. Cent. South Univ.* **2018**, *25*, 1948–1957. [CrossRef]
3. Doe, U. *Multiyear Research Development and Demonstration Plan: Planned Program Activities for 2011–2020*; Office DFCT, US Department of Energy: Washngton, DC, USA, 2017; pp. 3–4.
4. Arfeen, Z.A.; Abdullah, M.P.; Hassan, R.; Othman, B.M.; Siddique, A.; Rehman, A.U.; Sheikh, U.U. Energy storage usages: Engineering reactions, economic-technological values for electric vehicles—A technological outlook. *Int. Trans. Electr. Energy Syst.* **2020**, *30*, e12422. [CrossRef]
5. Kim, A.R.; Vinothkannan, M.; Ramakrishnan, S.; Park, B.-H.; Han, M.-K.; Yoo, D.J. Enhanced electrochemical performance and long-term durability of composite membranes through a binary interface with sulfonated unzipped graphite nanofibers for polymer electrolyte fuel cells operating under low relative humidity. *Appl. Surf. Sci.* **2022**, *593*, 153407. [CrossRef]
6. Meng, T.; Ciu, D.; Ji, Y.L. Optimization and efficiency analysis of methanol SOFC-PEMFC hybrid system. *Int. J. Hydrogen Energy* **2022**, *47*, 27690–27702. [CrossRef]
7. Chen, R.R.; Luo, Q.; Luo, X.L. Design and operation optimization of an on-site hydrogen production and purification integration system for PEMFC. *Fuel* **2024**, *370*, 131834. [CrossRef]
8. Li, X.; Wang, Y.D.; Zhan, M. Review on sealing materials for proton exchange membrane fuel cell. *J. Ship Electr. Technol.* **2020**, *6*, 19–23.
9. Ye, D.H.; Zhan, Z.G. A review on the sealing structures of membrane electrode assembly of proton exchange membrane fuel cells. *J. Power Sources* **2013**, *231*, 285–292. [CrossRef]
10. Qiu, D.; Peng, L.; Yi, P.; Lehnert, W.; Lai, X. Review on proton exchange membrane fuel cell stack assembly: Quality evaluation, assembly method, contact behavior and process design. *Renew. Sustain. Energy Rev.* **2021**, *152*, 111660. [CrossRef]
11. Song, K.; Wang, Y.; Ding, Y.; Mueller-Welt, P.; Stuermlinger, T. Assembly techniques for proton exchange membrane fuel cell stack: A literature review. *Renew. Sustain. Energy Rev.* **2022**, *153*, 111777. [CrossRef]

12. Tan, J.; Chao, Y.J.; Yang, M. Chemical and mechanical stability of a Silicone gasket material exposed to PEM fuel cell environment. *Int. J. Hydrogen Energy* **2011**, *36*, 1846–1852. [CrossRef]
13. Lin, C.W.; Chen, C.H.; Tan, J. Dynamic mechanical characteristics of five elastomeric gasket materials aged in a simulated and an accelerated PEM fuel cell environment. *Int. J. Hydrogen Energy* **2011**, *36*, 6756–6767. [CrossRef]
14. Xu, Y.; Li, X.B.; Zhou, Y.O. Persson's theory of purely normal elastic rough surface contact: A tutorial based on stochastic process theory. *Int. J. Solids Struct.* **2024**, *290*, 112684. [CrossRef]
15. Ma, B.; Jin, F.; Sun, Z. Leakage analysis of bolted flange joints considering surface roughness: A theoretical model. *Proc. Inst. Mech. Eng. Part E J. Process Mech. Eng.* **2017**, *232*, 203–233. [CrossRef]
16. Lorenz, B.; Persson, B.N. Leak rate of seals: Effective-medium theory and comparison with experiment. *Eur. Phys. J. E* **2010**, *31*, 159–167. [CrossRef] [PubMed]
17. Lorenz, B.; Persson, B.N. Leak rate of seals: Comparison of theory with experiment. *Europhys. Lett.* **2009**, *86*, 44006. [CrossRef]
18. Kucaba-Pietal, A. Scale effect in microflows modelling with the micropolar fluid theory. In Proceedings of the Scale Effect in Microflows Modelling with the Micropolar Fluid Theory, Crete Island, Greece, 5–10 June 2016.
19. Persson, B.N.J. Contact Mechanics for Randomly Rough Surfaces: On the Validity of the Method of Reduction of Dimensionality. *Tribol. Lett.* **2015**, *58*, 11. [CrossRef]
20. Scaraggi, M.; Persson, B.N.J. General contact mechanics theory for randomly rough surfaces with application to rubber friction. *J. Chem. Phys.* **2015**, *143*, 224111. [CrossRef] [PubMed]
21. Carral, C.; Mele, P. A numerical analysis of PEMFC stack assembly through a 3D finite element model. *Int. J. Hydrogen Energy* **2014**, *39*, 4516–4530. [CrossRef]
22. Habibnia, M.; Shakeri, M.; Nourouzi, S. Determination of the effective parameters on the fuel cell efficiency, based on sealing behavior of the system. *Int. J. Hydrogen Energy* **2016**, *41*, 18147–18156. [CrossRef]
23. Wei, C.; Wu, Z.; Jiang, D. Effect of temperature on output performance of proton exchange membrane fuel cell. *J. Renew. Energy Resour.* **2021**, *39*, 1588–1593.
24. Shizuku, F.; Okada, S.; Kajiwara, T. Fuel Cell Resin Frame Assembly. U.S. Patent No. 10,522,851, 31 December 2019.
25. Hübne, G. Membrane, Membrane-Electrode Assembly, Fuel Cell and Method for Prducing a Membrane. U.S. Patent No. 10,573,916, 25 February 2020.
26. Yoshida, H.; Wachi, D. Fuel Cell with a Seal Tightly in Contact with an Electrode for Preventing Leakage of a Reactant Gas. U.S. Patent No. 7,326,485, 15 February 2008.
27. Steinbach, A.J.L.; Debe, M.K. Gas Diffusion Layer Incorporating a Gasket. US Patent 7,732,083, 8 June 2010.
28. Yuan, X.Z.; Shi, Z.Q.; Song, J.C. MEA—Membrane Electrode Assembly. *Encycl. Energy Storage* **2022**, 276–289.
29. Shi, D.C.; Cai, L.; Zhang, C.Z. Fabrication methods, structure design and durability analysis of advanced sealing materials in proton exchange membrane fuel cells. *Chem. Eng. J.* **2023**, *454*, 139995. [CrossRef]
30. Zhang, S.H.; Wang, Z.H.; Zhang, R.L. Comprehensive study and optimization of membrane electrode assembly structural composition in proton exchange membrane water electrolyzer. *Int. J. Hydrogen Energy* **2023**, *48*, 35463. [CrossRef]
31. Ishikawa, H.; Teramoto, T.; Ueyama, Y. Use of a Sub-Gasket and Soft Gas Diffusion Layer to Mitigate Mechanical Degradation of a Hydrocarbon Membrane for Polymer Electrolyte Fuel Cells in Wet-Dry Cycling. *J. Power Sources* **2016**, *325*, 35–41. [CrossRef]
32. Jacobine, A.F.; Woods, J.G.; Nakos, S.T.; Burdzy, M.P.; Einsla, B.R.; Welch, K.J. UV-Curable Fuel Cell Sealants and Fuel Cells Formed Therefrom. US Patent 20090004541, 1 January 2009.
33. Chen, M.; Liu, M.J.; Feng, Y. Technical challenges and enhancement strategies for transitioning PEMFCs from H_2-air to H_2-O_2. *Energy Convers. Manag.* **2024**, *311*, 118525. [CrossRef]
34. Yin, J.; Yang, F.; Yang, D. Design and simulation of integrated seal for proton exchange membrane fuel cell. *J. Automob. Technol.* **2021**, *7*, 15–21.
35. Liang, P.; Qiu, D.K.; Peng, L.F. Structure failure of the sealing in the assembly process for proton exchange membrane fuel cells. *Int. J. Hydrogen Energy* **2017**, *42*, 10217–10227. [CrossRef]
36. Kömmling, A. Comparison of different test methods for lifetime prediction of O-ring seals. In Proceedings of the Polymer Degradation Discussion Group Conference, St. Julian, Malta, 1–5 September 2019.
37. Peng, L.; Liu, D.A.; Hu, P. Fabrication of metallic bipolar plates for proton exchange membrane fuel cell by flexible forming process-numerical simulations and experiments. *J. Fuel Cell Sci. Technol.* **2010**, *7*, 031009. [CrossRef]
38. Peng, L.; Lai, X.; Yi, P. Design, optimization, and fabrication of slotted-interdigitated thin metallic bipolar plates for PEM fuel cells. *J. Fuel Cell Sci. Technol.* **2010**, *8*, 011002. [CrossRef]
39. Choirotin, I.; Choiron, M.A. Defect Prediction at The Superplastic Forming Process of The Bipolar Plate by Simulation. *J. Energy Mech. Mater. Manuf. Eng.* **2018**, *3*, 49–54. [CrossRef]
40. Xu, Y.; Peng, L.; Yi, P. Analysis of the flow distribution for thin stamped bipolar plates with tapered channel shape. *Int. J. Hydrogen Energy* **2016**, *41*, 5084–5095. [CrossRef]
41. Tan, J.; Chao, Y.J.; Li, X. Degradation of silicone rubber under compression in a simulated. *PEM Fuel Cell Environ.* **2007**, *172*, 782–789.
42. Li, G.; Gong, J.M.; Tan, J.Z. Stress relaxation behavior and life prediction of gasket materials used in proton exchange membrane fuel cells. *J. Central South Univ.* **2019**, *26*, 623–631. [CrossRef]

43. Qiu, D.; Liang, P.; Peng, L.; Yi, P.; Lai, X.; Ni, J. Material behavior of rubber sealing for proton exchange membrane fuel cells. *Int. J. Hydrogen Energy* **2020**, *45*, 5465–5473. [CrossRef]
44. Wu, F.; Chen, B.; Pan, M. Degradation of the sealing silicone rubbers in a proton exchange membrane fuel cell at cold start conditions. *Int. J. Electrochem. Sci.* **2020**, *15*, 3013–3028. [CrossRef]
45. Chang, H.; Wan, Z.; Chen, X. Temperature and humidity effect on aging of silicone rubbers as sealing materials for proton exchange membrane fuel cell applications. *Appl. Therm. Eng.* **2016**, *104*, 472–478. [CrossRef]
46. Xia, L.; Wang, M.; Wu, H. Effects of cure system and filler on chemical aging behavior of fluoroelastomer in simulated proton exchange membrane fuel cell environment. *Int. J. Hydrogen Energy* **2016**, *41*, 2887–2895. [CrossRef]
47. Cleghorn, S.J.C.; Mayfield, D.K.; Moore, D.A. A polymer electrolyte fuel cell life test: 3 years of continuous operation. *J. Power Sources* **2006**, *158*, 446–454. [CrossRef]
48. Yang, Z.; Zhu, W.F.; Dong, R. Multi-scale dimensionless prediction model of PEMFC sealing interface leakage rate based on fractal geometry. *Int. J. Hydrogen Energy* **2023**, *48*, 5276–5287. [CrossRef]
49. Yang, Z.; Zhu, W.F.; Zhang, Q.Q. PEMFC sealing modeling relating to fractal characteristics of gasket-BPP interface based on micro-contact. *Int. J. Hydrogen Energy* **2024**, *63*, 803–814. [CrossRef]
50. Yang, C.; Persson, B.N.J. Contact mechanics: Contact area and interfacial separation from small contact to full contact. *J. Phys. Condens. Matter* **2008**, *20*, 13. [CrossRef]
51. Aweimer, A.S.O.; Bouzid, A.H. Evaluation of interfacial and permeation leaks in gaskets and compression packing. *J. Nucl. Eng. Radiat. Sci.* **2019**, *5*, 9. [CrossRef]
52. Husar, A.; Serra, M.; Kunusch, C. Description of gasket failure in a 7 cell PEMFC stack. *J. Power Sources* **2007**, *169*, 85–91. [CrossRef]
53. Chen, C.Y.; Su, S.C. Effects of assembly torque on a proton exchange membrane fuel cell with stamped metallic bipolar plates. *Energy* **2018**, *159*, 440–447. [CrossRef]
54. *ASTM D3078-02(2021)e1*; Standard Test Method for Determination of Leaks in Flexible Packaging by Bubble Emission. ASTM International: West Conshohocken, PA, USA, 2021.
55. Xu, Q.; Zhao, J.; Chen, Y. Effects of gas permeation on the sealing performance of PEMFC stacks. *Int. J. Hydrogen Energy* **2021**, *46*, 36424–36435. [CrossRef]
56. Qiu, D.K.; Peng, L.; Lai, X. Mechanical failure and mitigation strategies for the membrane in a proton exchange membrane fuel cell. *Renew. Sustain. Energy Rev.* **2019**, *113*, 109289. [CrossRef]
57. Hou, Y.; Zhou, W.; Shen, C. Experimental investigation of gas-tightness and electrical insulation of fuel cell stack under strengthened road vibrating conditions. *Int. J. Hydrogen Energy* **2011**, *36*, 13763–13768. [CrossRef]
58. Deshpande, J.; Dey, T.; Ghosh, P.C. Effect of vibrations on performance of polymer electrolyte membrane fuel cells. *Energy Procedia* **2014**, *54*, 756–762. [CrossRef]
59. Rajalakshmi, N.; Pandian, S.; Dathathreyan, K.S. Vibration Tests on a PEM Fuel Cell Stack Usable in Transport Application. *Int. J. Hydrogen Energy* **2009**, *34*, 3383–3387.
60. Cui, T.; Chao, Y.; Van Zee, J. Sealing force prediction of elastomeric seal material for PEM fuel cell under temperature cycling. *Int. J. Hydrogen Energy* **2014**, *39*, 1430–1438. [CrossRef]
61. Kim, T.; Nguyen, N.D.; Kim, Y.; Yu, S. Experimental investigation of time-dependent electrical load effects through multipoints in-situ measurement of temperature and relative humidity of PEMFC bipolar plate under transient operation. *Appl. Therm. Eng.* **2024**, *247*, 123049. [CrossRef]
62. Zhang, J.; Hu, Y. Sealing performance and mechanical behavior of PEMFCs sealing system based on thermodynamic coupling. *Int. J. Hydrogen Energy* **2020**, *45*, 23480–23489. [CrossRef]
63. Zhang, N.; Li, Q.; Hu, K. Compressive and Sealing Characteristics of PTFE under Cyclic Loading-unloading. *J. Wuhan Univ. Technol. Mater. Sci. Ed.* **2015**, *30*, 181–184. [CrossRef]
64. Pei, H.C.; Xing, L.; Chen, J.B. Visualisation study on water management of cathode dead-ended PEMFC under pressure-swing operation. *Prog. Nat. Sci. Mater. Int.* 2024, *in press*. [CrossRef]